ACS APPLIED MATERIALS & INTERFACES

Research Article

www.acsami.org

Highly Anti-UV Properties of Silk Fiber with Uniform and Conformal Nanoscale TiO_2 Coatings via Atomic Layer Deposition

Xingfang Xiao,[†,‡] Xin Liu,[†] Fengxiang Chen,[†,§] Dong Fang,[†] Chunhua Zhang,[†] Liangjun Xia,[†] and Weilin Xu*[,†,‡]

[†]Key Laboratory of Green Processing and Functional Textiles of New Textile Materials, Ministry of Science and Technology, Wuhan Textile University, Wuhan 430073, P. R. China

[‡]College of Material Science and Engineering, Wuhan Institute of Technology, Wuhan 430073, P. R. China

[§]Faculty of Materials Science and Engineering, Hubei University, Wuhan 430062, P. R. China

Supporting Information

ABSTRACT: In this study, silk fiber was successfully modified via the application of a nanoscale titania coating using atomic layer deposition (ALD), with titanium tetraisopropoxide (TIP) and water as precursors at 100 °C. Scanning electron microscopy, X-ray energy dispersive spectroscopy, X-ray photoelectron spectroscopy, transmission electron microscope, and field emission scanning electron microscope results demonstrated that uniform and conformal titania coatings were deposited onto the silk fiber. The thermal and mechanical properties of the TiO_2 silk fiber were then investigated. The results showed that the thermal stability and mechanical properties of this material were superior to those of the uncoated substance. Furthermore, the titania ALD process provided the silk fiber with excellent protection against UV radiation. Specifically, the TiO_2-coated silk fibers exhibited significant increases in UV absorbance, considerably less yellowing, and greatly enhanced mechanical properties compared with the uncoated silk fiber after UV exposure.

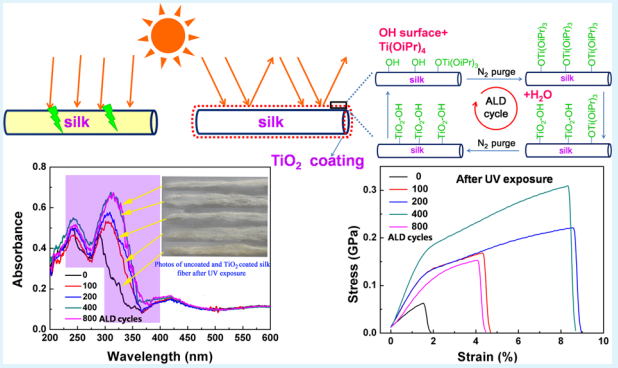

KEYWORDS: *atomic layer deposition, silk fiber, anti-UV properties, titania, nanoscale coatings*

1. INTRODUCTION

Silk is a natural protein filament that contains 18 amino acids. This material is known as the "queen of fibers" for its inherently elegant sheen, soft and smooth texture, excellent mechanical strength, high hygroscopicity, and its regeneration properties.[1−3] However, the protein nature of silk also yields inherent disadvantages, such as brittleness, yellowing, and even degradation caused by UV irradiation.[4−6] The latter is one of the most important defects affecting the end use of silk fiber. Currently, the textile industry has developed to the extent that it requires not only functional textile products with basic comfort and fashionableness, but also materials with added features. For example, textiles with anti-UV protection, self-cleaning capabilities, and antibacterial properties have high added value and are therefore in demand.[7] Thus, the production of silk fiber with superior properties for broad applications is highly desirable.

In order to improve the UV-protection functionality of textile fibers, considerable effort has been expended on fabricating anti-UV textile fibers. Organic−inorganic nanocomposites produced using in situ photoinitiation and disassembled TiO_2-clay composites with polymer have been prepared as UV-protection materials;[8] however, this method is unsuitable for application to natural fibers. Instead, coating the fabric with nanofunctional materials is one of the most effective methods to overcome intrinsic deficiencies and to introduce new properties to the final product. Previously, T. Lin et al.[9] have applied organic UV absorber-intercalated layered double hydroxides (LDHs) to cotton fabrics, yielding a dual-function coating with superhydrophobicity and UV-blocking characteristics. This was achieved using electrostatic layer-by-layer self-assembly technology. Finally, a 4-fold increase in the UV-protection ability of cotton fabrics was obtained. Through a titania sol−gel process, N. Abidi et al.[4,10] have reported successful titania-nanosol coating of cotton fabrics, which imparted cotton fabric with excellent self-cleaning and improved UV-protection properties. L. Wang et al.[11] have applied a ZnO@SiO_2 core−shell nanorod to cotton textiles in order to obtain superhydrophobic and ultraviolet-blocking properties. Similarly, M. Montazer et al.[12] have fabricated self-cleaning, antibacterial, and anti-UV wool and polyester fiber with nano-TiO_2 through enzymatic pretreatment. In a report by

Received: June 30, 2015
Accepted: September 10, 2015
Published: September 10, 2015

DOI: 10.1021/acsami.5b05868
ACS Appl. Mater. Interfaces 2015, 7, 21326−21333

G. Li et al.,[3] TiO_2 and TiO_2@Ag nanoparticles were assembled on silk fiber through covalent linkages, including enediol ligand−metal oxide bonding, resin dehydration, and the acylation of silk. UV-protection properties and antibacterial capability were then realized. Q. Li et al.[13] presented a process to synthesize single-phase anatase titanium dioxide nanocrystallites at room temperature imparting cotton fabric with self-cleaning and UV protection properties.

While these studies have exhibited some success, in many cases the methods outlined above damage the textile fiber, thereby degrading its inherent advantages. In other cases, the procedure is too cumbersome, or the adhesion between the coating and fiber is weak. An alternative approach to textile coating is to utilize chemical reactions within the silk fiber to form a uniform and conformal nanolayer in a relatively gentle environment. Atomic layer deposition (ALD) has recently emerged as a powerful technique for conformal coating on materials with outstanding advantages including excellent uniformity, precise thickness control, and high adhesion.[14−16] In the ALD process, the deposition of the two precursors is independent of the substrate composition and geometry; therefore, this technique has been widely used in various applications, including the wear-resistant coating of microelectromechanical devices,[17] optical and electric matrix modification,[18] efficient synergisitic microwave absorbers,[19,20] and the UV protection, wetting, toughness enhancement, and biocompatibility improvement of polymer fiber materials in particular.[21−24] To the best of our knowledge, few studies have been conducted on the production of anti-UV silk fiber with TiO_2 using the ALD technique.

In the present study, we deposited TiO_2 coating onto silk fiber to function as a UV absorber, using the ALD technique. The morphology, microstructure, thermal properties, mechanical properties, and UV protection of the TiO_2-coated silk fiber were characterized.

2. EXPERIMENTAL SECTION

2.1. Materials. The silk fibers used in this study had a linear density of 2.0−2.5 dtex and were purchased from Tongxiang Home Textile, Ltd. (Zhejiang, China). Prior to ALD, the silk fibers were degummed as follows: The silk fibers were first boiled in 0.06g/L soapy water (sodium carbonate solution) for 30 min and then washed in distilled water. These steps were repeated twice, and the fibers were then dried at 60 °C in an oven. For the ALD coating, titanium tetraisopropoxide (TIP) was purchased from Strem Chemicals, Inc., while deionized water (I degree, specific resistance is 10−16 MΩ cm at 25 °C) was produced by Molgeneral (Molecular).

2.2. TiO_2 ALD Coatings on Silk Fiber. The ALD process was conducted in a hot-wall closed chamber-type ALD reactor utilizing N_2 as a precursor carrier and purge gas. Prior to ALD processing, the prepared silk was placed in the ALD reactor and dried at 100 °C for 10 min in vacuum (20 Pa) with a steady N_2 gas stream (20 sccm). TiO_2 deposition was performed by introducing alternating doses of TIP and H_2O. To produce adequate vapor pressures, the TIP temperature was maintained at 60 °C, while the H_2O was fixed to room temperature. The delivery line from the precursor container to the reactor chamber was maintained at 100 °C, and the typical deposition temperature used in this study was 100 °C. A single TiO_2 ALD cycle was conducted according to the following sequence: TIP dose/N_2 purge/H_2O dose/N_2 purge. The ALD pulse, exposure, and purge times for the TIP were 0.2, 15, and 30 s, respectively, while those for the H_2O were 0.05, 15, and 30 s, respectively. In this study, silk fibers with four depositions, 100, 200, 400, and 800 cycles of TiO_2, were prepared.

The schematic process of TiO_2 ALD on silk fibers is shown in Figure 1. One ALD process cycle includes two half reactions: TIP reacts with the −OH surface, and water reacts with the $-OCH(CH_3)_2$

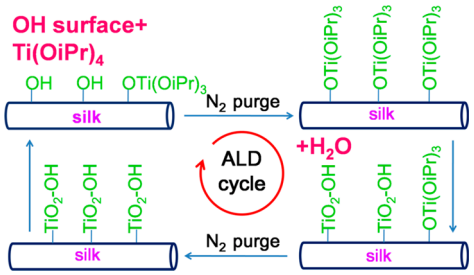

Figure 1. Schematic process of TiO_2 ALD on silk fibers.

surface. This occurs through sequential saturation exposures of the TIP and water, which are separated by N_2 purging steps. Then, the −OH surface is reproduced, and the ALD cycle is repeated, facilitating the layer-by-layer growth of the TiO_2 coating on the silk fiber.

2.3. UV Treatment of Silk Fiber. The uncoated and TiO_2 coated silk fibers were exposed to the UV light for 1 h. The distance to the UV light was fixed at 20 cm. UV ray intensity meter (TN-2340,TAINA, China) was used to measure the intensity of UV irradiation on silk fiber. The UV intensity on silk fiber was 19 000 μW/cm^2, which was far more than the intensity of sunshine.

2.4. Sample Characterization. Morphologies and structures of silk fibers were investigated using a scanning electron microscope (SEM) (JSM-7001F, JEOL Ltd., Japan) with an operating voltage of 20 kV. The elemental composition of samples was analyzed using an X-ray energy dispersive spectroscopy (EDS) detector (QX200, Bruker) attached to the SEM.

The crystal structures of samples were characterized by means of X-ray diffraction (XRD) on a D/MAX.RB diffractometer with Cu Ka radiation (l50.154 nm) at a generator voltage of 40 kV and a generator current of 40 mA.

Transmission electron microscope (TEM) (Tecnai G2 F30) was used to investigate the conformality, uniformity, and thickness of TiO_2 layers on silk fibers, with an accelerating voltage of 200 kV. Cross-sectional TEM samples were prepared by embedding silk fiber in resin. The embedded samples were then sectioned by microtome and attached to Cu grids using an adhesive.

Field emission scanning electron microscope (FESEM) (Quanta 250 FEG-INCA) was also used to investigate the ALD layer, with an accelerating voltage of 10 kV. The cross-section sample was fabricated using a focused ion beam (FIB) to cut a thin film along the radial direction of silk fiber. In order to protect the silk fiber, a carbon layer was plated on the silk fiber before using FIB.

X-ray photoelectron spectroscopy (XPS) (Kratos AXIS Ultra XPS) was used to investigate the chemical composition on the silk fiber substrates. XPS measurements were operated at 15 kV using a monochromated Al source that can give an energy resolution of 1 eV with a dwell time of 200 ms. The scans was carried out from 1197 to −3 eV to collect XPS spectra. High-resolution detail scans were performed around peaks of interest.

Thermogravimetry analysis (TGA) was carried out using a TG 209 F1 (NETZSCH Instruments Co., Ltd.) thermogravimetric analyzer from room temperature to 900 °C with a heating rate of 10 °C/min in N_2.

UV−vis spectrophotometer (Lambda 35, PerkinElmer) was used to test the absorbance spectra of silk fiber with and without TiO_2 ALD coatings.

The optical photographs of the silk fibers with and without TiO_2 ALD coatings after UV treatment were measured by a digital camera (Canon, EOS 70D).

The mechanical properties of silk fibers were measured with a universal materials testing machine (Instron 5566) at 20 °C and relative humidity of 63% at a gauge length 10 mm and strain rate of 10 mm/min. Specimens including silk fiber treated with different TiO_2 ALD cycles before and after UV exposure were cut into at a length of 50 mm. The stress−strain curves for the specimens were obtained from the recorded load deformation curves. The tensile stress, strain to failure, and fracture work values are the average of 20 measurements.

DOI: 10.1021/acsami.5b05868
ACS Appl. Mater. Interfaces 2015, 7, 21326−21333

3. RESULTS AND DISCUSSION

Figure 2 shows the SEM images and EDS curves of control uncoated silk fibers and silk fibers coated with 800 cycles of

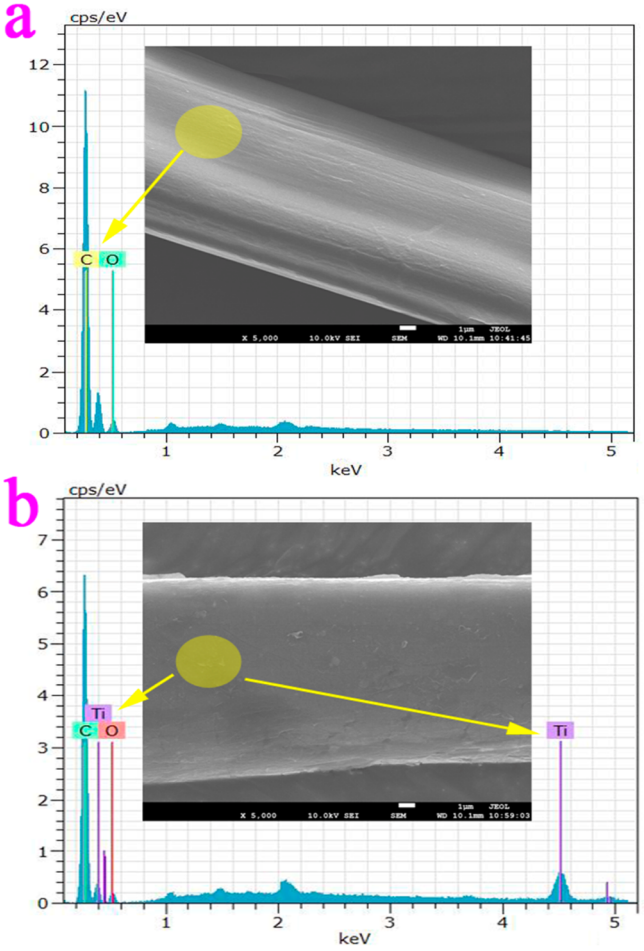

Figure 2. SEM images and EDS curves of (a) control uncoated silk fibers and (b) 800-cycle TiO_2-coated silk fibers.

TiO_2 at 100 °C. The surfaces of the control silk fiber (Figure 2a) and ALD-coated silk fiber (Figure 2b) are identical, which is consistent with the previous finding that the ALD process can prepare conformal film on a substrate.[14] The EDS curves confirm that the Ti is present on the ALD-coated silk fiber surfaces.

In order to confirm that the TiO_2 ALD film was coated on the silk, the uncoated and ALD-coated fibers were calcined in a muffle at 600 °C for 5 h. Eventually, the uncoated silk fiber was completely burned away, while the ALD-coated fiber retained the silk fiber structure. It has been suggested the titania replica fiber can be obtained in this manner.[25] Figure 3 shows the SEM image (Figure 3a) and XRD pattern of a TiO_2 replica (Figure 3b) where the 800 cycles of TiO_2 film were deposited at 100 °C and the silk fiber was removed by air-annealing at 600 °C for 5 h, and XRD patterns of the ALD-coated fibers (Figure 3c). As shown in Figure 3a, these fibers retained the original fibrous silk morphology with silk body removal, and it is apparent that the titania replicas have hollow interiors. Further, it can be seen from Figure 3b that the sample exhibits a well-crystallized anatase crystalline phase (space group (SG): $I4_1/amd$; JCPDS No. 21-1272), and no peaks for other impurities, which indicates that anatase has been produced. The XRD results

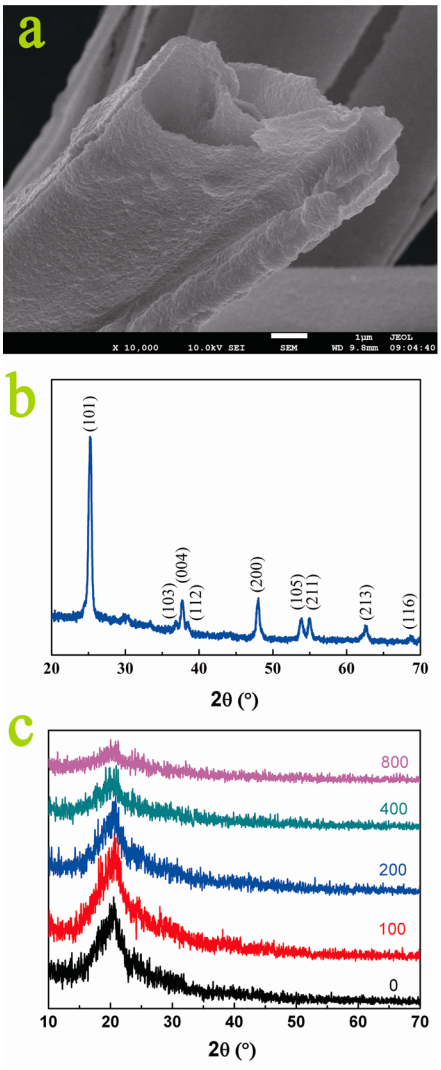

Figure 3. (a) SEM image and (b) XRD pattern of a TiO_2 replica where the 800 cycles of TiO_2 film were deposited at 100 °C and the silk fiber was removed by air-annealing at 600 °C for 5 h, and (c) XRD spectra of uncoated (0 cycle) and 100-, 200-, 400-, 800-cycle TiO_2-coated silk fibers.

confirm that the ALD coating on the silk fiber was TiO_2. The XRD spectra of TiO_2-coated silk fiber treated with different cycles are shown in Figure 3c. The results show that there are no typical diffraction peaks for anatase or rutile TiO_2 on the TiO_2-coated silk fiber. With a combination of the XRD results and the ALD temperature (100 °C) used in this paper, the original TiO_2 before calcinations was an amorphous film.

To further investigate the conformality, uniformity, and thickness of TiO_2 ALD layers on silk fibers, a TEM image of 800-cycle TiO_2-coated silk fiber is shown in Figure 4a. The cross-sectional image shows a conformal and uniform coating of the silk fiber surface. The thickness is ~200 nm. However, there are still some discontinuities of the TiO_2 layer, which should be attributed to fracture during the TEM preparation. As silk fiber is an elastomer, it would deform in the process of curing or microtome cutting, which caused these discontinuities of the TiO_2 layer before TEM measurement. Therefore, the cross-section of ALD coatings on 400-cycle TiO_2-coated silk fiber is shown in Figure 4b. It is clear that a conformal and uniform film ~100 nm in thickness can be observed in FESEM

DOI: 10.1021/acsami.5b05868
ACS Appl. Mater. Interfaces 2015, 7, 21326−21333

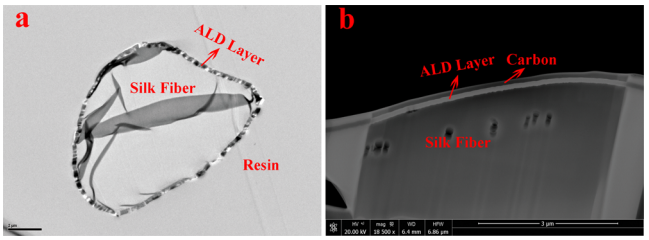

Figure 4. (a) TEM image of 800-cycle TiO_2-coated silk fiber and (b) FESEM image of 400-cycle TiO_2-coated silk fiber.

images. These results suggest that the conformal and uniform nanoscale ALD coatings could be deposited on silk fibers successfully.

The thickness of the ALD film also indicated that the growth rate of the ALD film was approximately 2.5 Å/cycle. For the conditions used here, the growth rate was greater than the 1 Å/cycle rate measured for TiO_2 films grown on silicon under the same conditions. Generally, during each deposition cycle on a silk fiber substrate, the precursor, reagent, and reaction products must follow a higher tortuous path through the substrate in order to reach or be removed from the growth surface. In addition, any molecules remaining in the fiber matrix after the gas purge step can cause excess growth in the subsequent cycle, compared with the case of planar silicon.[26] However, the results demonstrate that the growth rate observed in this study is acceptable for nanoscale uniform and conformal ALD film to be obtained.

To further investigate the chemical composite of the ALD coatings, XPS spectra were collected for uncoated silk fiber and coated silk fiber samples that underwent different numbers of ALD cycles. The survey scan in Figure 5 confirms the presence

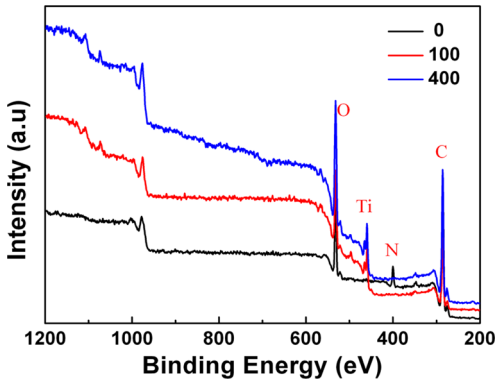

Figure 5. XPS survey scans for uncoated (0-cycle) and 100-, 400-cycle TiO_2-coated silk fibers.

of C, N, and O in the uncoated silk fiber, while C, O, and Ti elements are found in the ALD-coated silk fibers. High-resolution detail scans (Figure 6) were performed around peaks of interest, specifically, O 1s, N 1s, C 1s, and Ti 2p.

Figure 6a shows a high-resolution spectrum of the O 1s signal. For an untreated silk fiber, this signal is consistent with the expected peak position for absorbed water, C═O, or C—O bonds at 531.5 eV.[27,28] For the ALD-coated silk fiber, a signal becomes visible at 530 eV, corresponding to the O 1s from the TiO_2 surface layer.[29,30]

The N 1s spectrum is shown in Figure 6b. The uncoated silk fiber exhibits a large N 1s feature. However, the N 1s signal has almost disappeared after the ALD process, which is consistent with the fiber surface being coated by the TiO_2.The N 1s peak at 399.5 eV is due to the N—O and N—C bonds.[31]

The XPS spectrum of the C 1s peak is shown in Figure 6c. The C 1s fine scan contains two distinct peaks: an intense peak at 284.5 eV, which is associated with the C—C bonds, and a small peak at 288.5 eV that corresponds to C═O or C—O bonds.[27,32] The different peak intensities of the TiO_2-coated silk may be ascribed to the different absorbency of TIP.

Figure 6d shows a detailed spectrum of the Ti 2p signal. It can be seen that two clear Ti 2p peaks emerge for the ALD-coated silk, which are not present for the uncoated fiber. These two peaks are at 458.5 and 464 eV, and are therefore assigned to Ti $2p_{3/2}$ and Ti $2p_{1/2}$, respectively, which are typical XPS spectra of Ti^{4+}.[33] As expected, the more ALD cycles of TiO_2 that are performed, the stronger the obtained peak intensity. The XPS data thus reinforce the finding that TiO_2 coatings were successfully deposited onto the silk fiber using ALD.

The thermogravimetric (TG) and derivative thermogravimetry (DTG) curves of the uncoated silk fiber and TiO_2-coated silk fiber are shown in Figure 7. Further, the thermal analysis data from Figure 7 are listed in Table 1. The TG curves of the uncoated and TiO_2-coated samples exhibit similar temperature ranges with the following three mass-loss processes: (1) 30–205 °C, which is the initial stage mass loss, which is attributed to the loss of the absorbed moisture from the silk fiber; (2) 205–390 °C, which is the major decomposition stage, which indicates silk fiber decomposed into small molecules; (3) 390–900 °C, which is the third stage, and is primarily caused by char decomposition of the silk fiber. However, the mass loss between the uncoated and TiO_2-coated silk fibers differs, and also decreases as the TiO_2 ALD cycle increases, as shown in Figure 7 and Table 1. In particular, the mass loss of the silk fiber coated with 800 cycles of TiO_2 deposition is 10.1% greater than that of the uncoated samples, which is clearly due to the TiO_2 coated on the silk fiber. The two peaks of the DTG curves in Figure 7 correspond to the moisture loss and decomposition of the silk fiber. The DTG curves and Table 1 indicate that the fastest mass loss temperature of the TiO_2-coated samples is higher than that of the uncoated sample, and the temperature increases as the TiO_2 ALD cycle increases. For the 800-cycle TiO_2-coated silk fiber, the fastest mass loss temperature of the uncoated silk fiber is increased from 304.5 to 312.0 °C. This may be attributed to the high melting temperature of the TiO_2 ALD coatings, which indicates that the thermal properties of TiO_2-coated silk fibers are more stable than those of uncoated silk fiber.

Combining the SEM, EDS, XRD, XPS, and TG analysis results, we can confirm the successful deposition of TiO_2 film on the silk fiber, and the thickness of the TiO_2 film increases as the ALD cycle number is increased.

The UV absorbance spectra of the uncoated and TiO_2-coated silk fibers and photographs of these fibers after UV exposure are shown in Figure 8. As shown in this figure, the UV absorbance (280–400 nm) of the TiO_2-coated silk fiber is higher than that of the uncoated silk fiber, and coating-cycle-dependent absorbance is observed for the TiO_2. Moreover, it can be seen that the characteristic absorbance peak of the TiO_2-coated silk fiber exhibits a bathochromic shift effect, and the intensity is higher than that of the uncoated silk fiber in the UV region. This is because both the silk fiber and TiO_2 ALD coating have the effect of absorbing UV irradiation; also, the TiO_2 ALD coatings have considerably stronger UV absorption. These results indicate that the TiO_2 coatings can effectively absorb the

DOI: 10.1021/acsami.5b05868
ACS Appl. Mater. Interfaces 2015, 7, 21326–21333

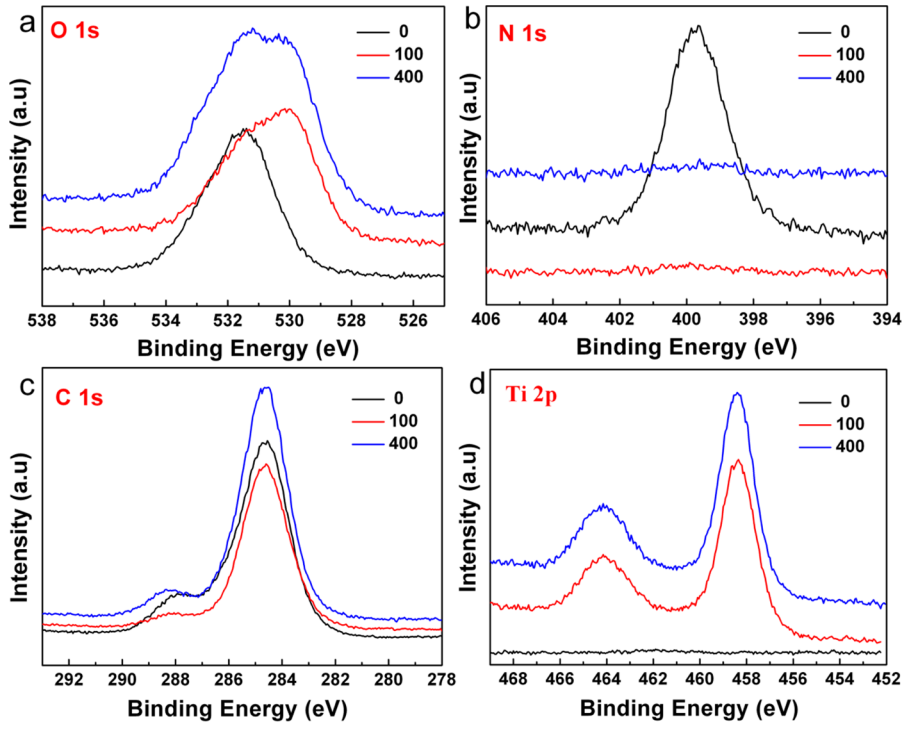

Figure 6. High-resolution detail scans of (a) O 1s, (b) N 1s, (c) C 1s, and (d) Ti 2p for uncoated (0 cycle) and 100-, 400-cycle TiO_2-coated silk fibers.

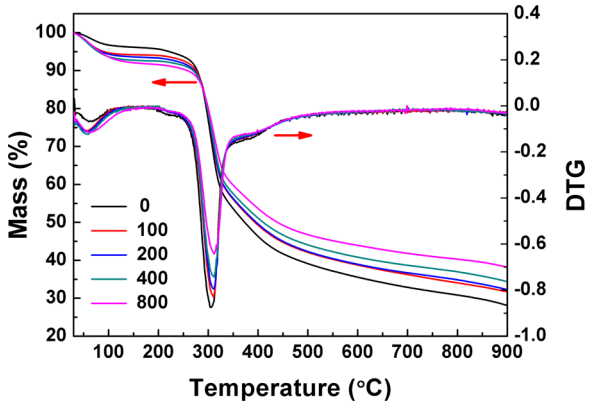

Figure 7. TG and DTG curves of uncoated (0-cycle) and 100-, 200-, 400-, 800-cycle TiO_2-coated silk fibers.

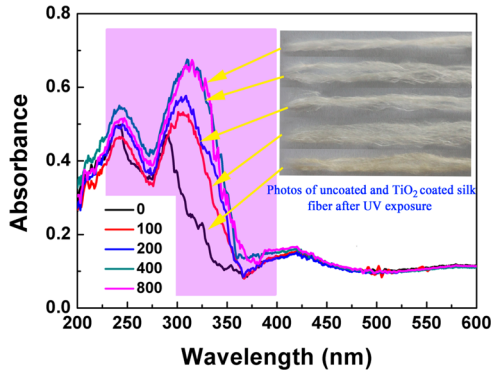

Figure 8. UV absorbance spectra of uncoated (0-cycle), 100-, 200-, 400-, 800-cycle TiO_2-coated silk fibers and photographs of these fibers after UV exposure.

Table 1. Thermal Analysis Data from TG and DTG Curves of Uncoated and TiO_2 Coated Silk Fiber[a]

silk fiber	uncoated	100 cycles TiO_2	200 cycles TiO_2	400 cycles TiO_2	800 cycles TiO_2
mass loss (%)	71.9	68.3	67.7	65.6	61.8
T_{max} (°C)	304.5	310.5	311.5	311.5	312.0

[a]Note that T_{max} is the fastest mass loss temperature.

UV irradiation, thus preventing direct exposure of the silk fiber to the UV radiation. From the photographs of silk (Figure 8), it can be seen that the high-intensity UV treatment caused a dramatic change in the color of the uncoated silk fiber, resulting in a dark yellow hue. The silk fiber coated with 100-cycle TiO_2 also exhibits visible yellowing, which suggests that the thickness of the ALD coating is insufficient to protect the silk fiber from discoloration due to UV irradiation. However, the silk fiber coated with 200-, 400-, and 800-cycle ALD coating exhibits a relatively white color. These color changes indicate the TiO_2 ALD coating can decrease the yellowing of the silk fiber after UV treatment.

Knowledge of the material mechanical properties is important for evaluating the performance of the silk fiber under practical application. Average values for the tensile stress, strain-to-failure, and work-of-fracture of both the uncoated and coated silk fibers are shown in Table 2. The uncoated silk fiber exhibits a tensile stress of 0.26 GPa and 18.27% strain-to-failure, whereas these values are slightly higher for the TiO_2-coated silk fiber. The work-of-fracture effectively illustrates the toughness and durability of the fiber. Compared to the uncoated silk, with a work-of-fracture of 0.28 cN/dtex, the 400-cycle TiO_2-coated silk exhibits an increase to 0.41 cN/dtex. Hence, taking sampling errors into account, the mechanical properties of the silk fibers are, in general, slightly increased by the ALD process.

DOI: 10.1021/acsami.5b05868
ACS Appl. Mater. Interfaces 2015, 7, 21326−21333

Table 2. Mechanical Properties of Silk Fiber before UV Exposure

silk fiber	tensile stress (GPa)	strain to failure (%)	fracture work (cN/dtex)
uncoated	0.26 ± 0.08	18.27 ± 2.83	0.28 ± 0.11
100-cycle TiO_2	0.30 ± 0.08	19.92 ± 3.11	0.35 ± 0.10
200-cycle TiO_2	0.28 ± 0.07	20.37 ± 4.01	0.31 ± 0.04
400-cycle TiO_2	0.31 ± 0.05	23.34 ± 3.75	0.41 ± 0.06
800-cycle TiO_2	0.29 ± 0.08	18.84 ± 4.25	0.32 ± 0.13

The mechanical properties of the silk fiber after high-intensity UV exposure were examined in order to explore the UV-protection ability of the TiO_2 ALD coating (Table 3).

Table 3. Mechanical Properties of Silk Fiber after UV Exposure

silk fiber	tensile stress (GPa)	strain to failure (%)	fracture work (cN/dtex)
uncoated	0.08 ± 0.02	1.27 ± 0.30	0.01 ± 0
100-cycle TiO_2	0.16 ± 0.04	4.11 ± 0.67	0.04 ± 0.01
200-cycle TiO_2	0.22 ± 0.05	7.19 ± 1.02	0.09 ± 0.02
400-cycle TiO_2	0.28 ± 0.09	8.85 ± 1.13	0.16 ± 0.07
800-cycle TiO_2	0.16 ± 0.03	4.32 ± 0.91	0.04 ± 0.01

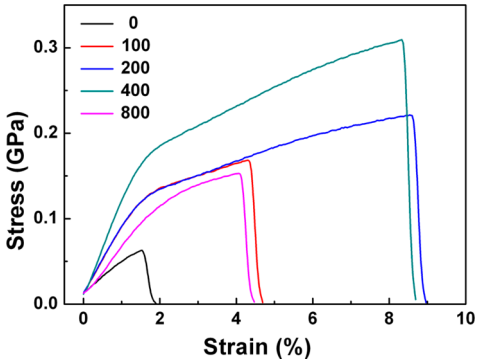

Figure 9. Stress–strain curves of uncoated (0 cycle) and 100-, 200-, 400-, 800-cycle TiO_2-coated silk fibers after UV exposure.

Figure 9 shows the typical stress–strain curves of uncoated and TiO_2-coated silk fiber after UV exposure. It can be seen in Table 3, after exposure to UV radiation for 1 h, that the tensile stress decreases to 0.08 GPa, the strain-to-failure decreases to 1.27%, and the work-of-fracture decreases to 0.01 cN/dtex. Thus, a sharp decrease can be seen in the mechanical properties of the uncoated silk fiber following the UV treatment. However, in comparison with the uncoated silk fiber, the TiO_2-coated silk samples exhibit a remarkably higher tensile stress and strain-to-failure after the UV treatment. Even in the case of the silk fiber coated with 100-cycle TiO_2, the resistance to the UV radiation is pronounced, resulting in increases in tensile stress and strain-to-failure of 100% and 127%, respectively, compared to the uncoated control fibers. In particular, the tensile strength, strain-to–failure, and work-of-fracture of the 400-cycle TiO_2-coated silk fiber increase 2.5-fold (from 0.08 to 0.28 GPa), 6.0-fold (from 1.27% to 8.85%), and 15-fold (from 0.01 to 0.16 cN/dtex) compared with the uncoated silk fiber after UV exposure, respectively. Although the mechanical properties are smaller than those of the silk fiber before UV exposure, the results clearly indicate that the TiO_2 ALD coating can effectively protect the mechanical properties of silk fiber from UV irradiation.

The macromolecular chain of the silk fiber consists of amino acid through the condensation of peptide bonds. When the silk fibers are exposed to UV radiation, a photochemical reaction occurs between the amino acid and radiation. This causes the UV radiation to be absorbed by the silk fiber. However, the photochemical reaction results in the destruction of the peptide, the degradation of the molecular chain, and significant degradation of the mechanical properties. In addition, the reaction intermediate causes yellowing of the silk fiber. The ALD process creates tight nanoscale coatings with strong chemical bonds between layers, unlike the coatings assembled through physical adhesion by traditional methods; thus, strong interactions between the silk fiber and TiO_2 layer are formed. Nano-TiO_2 is one of the most important UV shielding agents, and has effective shielding capacity against UVA and UVB. As shown in Figures 8 and 9, the yellowing resistance and mechanical properties of TiO_2-coated silk fibers are significantly better than those of the uncoated material, when the silk fibers are exposed to the UV radiation. This can be ascribed to the fact that the TiO_2 ALD coatings absorb and reflect the UV radiation. Furthermore, the UV-protection properties are gradually enhanced as the number of ALD cycles is increased to 400. However, the mechanical properties of 400-cycle TiO_2-coated silk fiber are better than the 800-cycle TiO_2-coated silk fiber after UV exposure. In order to investigate this phenomenon, the high-resolution SEM images of 400-cycle TiO_2-coated and 800-cycle TiO_2-coated silk fiber were characterized. As shown in Figure 10, it can be seen that

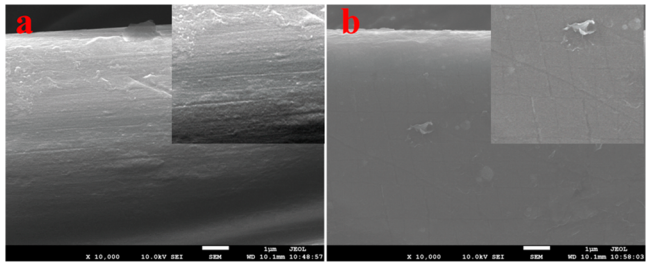

Figure 10. SEM images of (a) 400-cycle TiO_2-coated silk fiber and (b) 800-cycle TiO_2-coated silk fiber.

there are some microscopic cracks on the surface of 800-cycle TiO_2-coated silk fiber but not on that of 400-cycle TiO_2-coated silk fiber. As the cycle number of TiO_2 increases to 800, the TiO_2 film thickness is over thick, and the film becomes brittle. Thus, it is easy for microscopic cracks to emerge in the TiO_2 film during the ALD process of fiber moving and vibrating under the airflow. When the 800-cycle TiO_2-coated silk fiber is exposed to UV, part of the UV radiation could pass through these microscopic cracks and photocatalytically degrade the silk proteins, which causes the decrease of mechanical properties of the TiO_2-coated silk fiber. Therefore, the thickness of the 400-cycle deposited TiO_2 layer is sufficient to facilitate the UV

DOI: 10.1021/acsami.5b05868
ACS Appl. Mater. Interfaces 2015, 7, 21326–21333

protection, and a further increase in the thickness of the ALD coating is, therefore, unnecessary.

4. CONCLUSIONS

In summary, we successfully deposited the TiO_2 coating onto silk fiber via an ALD approach. SEM, TEM, and FESEM images revealed that uniform and conformal coatings were achieved on the silk fiber, and the chemical nature of the TiO_2 ALD coating was confirmed through XRD, EDS, and XPS analysis. The increase of the fastest mass loss temperature indicated by the TG and DTG measurements suggest superior thermal stability of theTiO_2-coated silk compared to that of the uncoated fiber, and the decrease in mass loss indicated by the TG in response to increased ALD cycle number indicates that the ALD process yields typical ALD growth behavior. The excellent UV protection properties of the TiO_2 ALD-coated silk fiber are manifest in the superior UV absorbance, minimal yellowing, and greatly enhanced mechanical properties, compared to the uncoated silk fiber after UV exposure. On the basis of these findings, it can be concluded that the deposition of nanoscale TiO_2 film on silk fiber through ALD is a very promising approach to modifying silk for enhanced UV protection. Furthermore, this method can be extended and used to deposit a wide range of coatings on fiber for use in various applications.

■ ASSOCIATED CONTENT

Supporting Information

The Supporting Information is available free of charge on the ACS Publications website at DOI: 10.1021/acsami.5b05868.

FTIR spectra of uncoated and TiO_2-coated silk fibers (PDF)

■ AUTHOR INFORMATION

Corresponding Author

*E-mail: weilin-xu@hotmail.com. Phone: +86 02759367690. Fax: +86 02759367690.

Notes

The authors declare no competing financial interest.

■ ACKNOWLEDGMENTS

We greatly acknowledge the support from the National Funds for Distinguished Young Scientists (Project No. 51325306, 51203124) and Major State Basic Research Development Program (973 Program) (Project No. 2012CB722701). The authors are grateful to Professor Yong Qin (Institute of Coal Chemistry, Chinese Academy of Sciences) for help with the ALD apparatus and for his valuable advice.

■ REFERENCES

(1) Baltova, S.; Vassileva, V. Photochemical Behaviour of Natural Silk-II. Mechanism of Fibroin Photodestruction. *Polym. Degrad. Stab.* **1998**, *60*, 61−65.

(2) Rajkhowa, R.; Gupta, V.; Kothari, V. Tensile Stress-strain and Recovery Behavior of Indian Silk Fibers and Their Structural Dependence. *J. Appl. Polym. Sci.* **2000**, *77*, 2418−2429.

(3) Li, G.; Liu, H.; Zhao, H.; Gao, Y.; Wang, J.; Jiang, H.; Boughton, R. Chemical Assembly of TiO_2 and TiO_2@ Ag Nanoparticles on Silk Fiber to Produce Multifunctional Fabrics. *J. Colloid Interface Sci.* **2011**, *358*, 307−315.

(4) Abidi, N.; Hequet, E.; Tarimala, S.; Dai, L. L. Cotton Fabric Surface Modification for Improved UV Radiation Protection Using Sol-gel Process. *J. Appl. Polym. Sci.* **2007**, *104*, 111−117.

(5) Wang, S.; Zhang, Y. Preparation of the Silk Fabric with Ultraviolet Protection and Yellowing Resistance Using TiO_2/La (III) Composite Nanoparticles. *Fibers Polym.* **2014**, *15*, 1129−1136.

(6) Lu, Z.; Mao, C.; Meng, M.; Liu, S.; Tian, Y.; Yu, L.; Sun, B.; Li, C. M. Fabrication of CeO_2 Nanoparticle-modified Silk for UV Protection and Antibacterial Applications. *J. Colloid Interface Sci.* **2014**, *435*, 8−14.

(7) Cakır, B. A.; Budama, L.; Topel, Ö.; Hoda, N. Synthesis of ZnO Nanoparticles Using PS-b-PAA Reverse Micelle Cores for UV Protective, Self-cleaning and Antibacterial Textile Applications. *Colloids Surf., A* **2012**, *414*, 132−139.

(8) Liao, C.; Wu, Q.; Su, T.; Zhang, D.; Wu, Q.; Wang, Q. Nanocomposite Gels via in Situ Photoinitiation and Disassembly of TiO_2-Clay Composites with Polymers Applied as UV Protective Films. *ACS Appl. Mater. Interfaces* **2014**, *6*, 1356−1360.

(9) Zhao, Y.; Xu, Z.; Wang, X.; Lin, T. Superhydrophobic and UV-blocking Cotton Fabrics Prepared by layer-by-layer Assembly of Organic UV Absorber Intercalated Layered Double Hydroxides. *Appl. Surf. Sci.* **2013**, *286*, 364−370.

(10) Abidi, N.; Cabrales, L.; Hequet, E. Functionalization of a Cotton Fabric Surface with Titania Nanosols: Applications for Self-cleaning and UV-protection Properties. *ACS Appl. Mater. Interfaces* **2009**, *1*, 2141−2146.

(11) Wang, L.; Zhang, X.; Li, B.; Sun, P.; Yang, J.; Xu, H.; Liu, Y. Superhydrophobic and Ultraviolet-blocking Cotton Textiles. *ACS Appl. Mater. Interfaces* **2011**, *3*, 1277−1281.

(12) Zheng, Y.; Xiao, M.; Jiang, S.; Ding, F.; Wang, J. Coating Fabrics with Gold Nanorods for Colouring, UV-protection, and Antibacterial Functions. *Nanoscale* **2013**, *5*, 788−795.

(13) Qi, K.; Xin, J. H. Room-temperature Synthesis of Single-phase Anatase TiO_2 by Aging and Its Self-cleaning Properties. *ACS Appl. Mater. Interfaces* **2010**, *2*, 3479−3485.

(14) George, S. M. Atomic Layer Deposition: An Overview. *Chem. Rev.* **2010**, *110*, 111−131.

(15) Knez, M.; Nielsch, K.; Niinistö, L. Synthesis and Surface Engineering of Complex Nanostructures by Atomic Layer Deposition. *Adv. Mater.* **2007**, *19*, 3425−3438.

(16) Marichy, C.; Bechelany, M.; Pinna, N. Atomic Layer Deposition of Nanostructured Materials for Energy and Environmental Applications. *Adv. Mater.* **2012**, *24*, 1017−1032.

(17) Mayer, T. M.; Elam, J. W.; George, S. M.; Kotula, P. G.; Goeke, R. S. Atomic-layer Deposition of Wear-resistant Coatings for Microelectro Mechanical Devices. *Appl. Phys. Lett.* **2003**, *82*, 2883−2885.

(18) Qin, Y.; Liu, L.; Yang, R.; Gosele, U.; Knez, M. Genernal Gssembly Method for Linear Metal Nanoparticle Chains Embedded in Nanotubes. *Nano Lett.* **2008**, *8*, 3221−3225.

(19) Wang, G.; Gao, Z.; Wan, G.; Lin, S.; Yang, P.; Qin, Y. High Densities of Magnetic Nanoparticles Supported on Graphene Fabricated by Atomic Layer Deposition and Their Use as Efficient Synergistic Microwave Absorbers. *Nano Res.* **2014**, *7*, 704−716.

(20) Wang, G.; Gao, Z.; Tang, S.; Chen, C.; Duan, F.; Zhao, S.; Lin, S.; Feng, Y.; Zhou, L.; Qin, Y. Microwave Absorption Properties of Carbon Nanocoils Coated with Highly Controlled Magnetic Materials by Atomic Layer Deposition. *ACS Nano* **2012**, *6*, 11009−11017.

(21) Hyde, G. K.; McCullen, S. D.; Jeon, S.; Stewart, S. M.; Jeon, H.; Loboa, E. G.; Parsons, G. N. Atomic Layer Deposition and Biocompatibility of Titanium Nitride Nano-coatings on Cellulose Fiber Substrates. *Biomed. Mater.* **2009**, *4*, 025001-1−025001-10.

(22) Hyde, G. K.; Scarel, G.; Spagnola, J. C.; Peng, Q.; Lee, K.; Gong, B.; Roberts, K. G.; Roth, K. M.; Hanson, C. A.; Devine, C. K.; Stewart, S. M.; Hojo, D.; Na, J.-S.; Jur, J. S.; Parsons, G. N. Atomic Layer Deposition and Abrupt Wetting Transitions on Nonwoven Polypropylene and Woven Cotton Fabrics. *Langmuir* **2010**, *26*, 2550−2558.

(23) Petrochenko, P. E.; Scarel, G.; Hyde, G. K.; Parsons, G. N.; Skoog, S. A.; Zhang, Q.; Goering, P. L.; Narayan, R. J. Prevention of Ultraviolet (UV)-induced Surface Damage and Cytotoxicity of Polyethersulfone Using Atomic Layer Deposition (ALD) Titanium Dioxide. *JOM* **2013**, *65*, 550−556.

DOI: 10.1021/acsami.5b05868
ACS Appl. Mater. Interfaces 2015, 7, 21326−21333

(24) Lee, S. M.; Pippel, E.; Gosele, U.; Dresbach, C.; Qin, Y.; Chandran, C. V.; Brauniger, T.; Hause, G.; Knez, M. Greatly Increased Toughness of Infiltrated Spider Silk. *Science* **2009**, *324*, 488−492.
(25) Wang, Y.; Liu, Z.; Han, B.; Sun, Z.; Du, J.; Zhang, J.; Jiang, T.; Wu, W.; Miao, Z. Replication of Biological Organizations Through a Supercritical Fluid Route. *Chem. Commun.* **2005**, 2948−2950.
(26) Hyde, G. K.; Park, K. J.; Stewart, S. M.; Hinestroza, J. P.; Parsons, G. N. Atomic Layer Deposition of Conformal Inorganic Nanoscale Coatings on Three-dimensional Natural Fiber Systems: Effect of Surface Topology on Film Growth Characteristics. *Langmuir* **2007**, *23*, 9844−9849.
(27) Beamson, G.; Briggs, D. High Resolution XPS of Organic Polymers; Wiley: Chichester, England, 1992; p 295.
(28) Yeqiu, L.; Jinlian, H.; Yong, Z.; Zhuohong, Y. Surface Modification of Cotton Fabric by Grafting of Polyurethane. *Carbohydr. Polym.* **2005**, *61*, 276−280.
(29) Ni, C.; Zhang, Z.; Wells, M.; Beebe, T. P.; Pirolli, L.; De Leo, L. P. M.; Teplyakov, A. V. Effect of Film Thickness and the Presence of Surface Fluorine on the Structure of a Thin Barrier Film Deposited from Tetrakis-(dimethylamino)-titanium onto a SiO_2 Substrate. *Thin Solid Films* **2007**, *515*, 3030−3039.
(30) Vesel, A.; Mozetic, M.; Kovac, J.; Zalar, A. XPS Study of the Deposited Ti Layer in a Magnetron-type Sputter Ion Pump. *Appl. Surf. Sci.* **2006**, *253*, 2941−2946.
(31) Hyde, G. K.; McCullen, S. D.; Jeon, S.; Stewart, S. M.; Jeon, H.; Loboa, E. G.; Parsons, G. N. Atomic Layer Deposition and Biocompatibility of Titanium Nitride Nano-coatings on Cellulose Fiber Substrates. *Biomed. Mater.* **2009**, *4*, 025001.
(32) Mitchell, R.; Carr, C.; Parfitt, M.; Vickerman, J.; Jones, C. Surface Chemical Analysis of Raw Cotton Fibres and Associated Materials. *Cellulose* **2005**, *12*, 629−639.
(33) Erdem, B.; Hunsicker, R. A.; Simmons, G. W.; Sudol, E. D.; Dimonie, V. L.; El-Aasser, M. S. XPS and FTIR Surface Characterization of TiO_2 Particles Used in Polymer Encapsulation. *Langmuir* **2001**, *17*, 2664−2669.

DOI: 10.1021/acsami.5b05868
ACS Appl. Mater. Interfaces 2015, 7, 21326−21333